Earthquakes and Structures, *Vol. 18, No. 3 (2020) 391-405*
DOI: https://doi.org/10.12989/eas.2020.18.3.391

Seismic resilience evaluation of RC-MRFs equipped with passive damping devices

Puteri Nihal Che Kamaludin[1a], Moustafa Moufid Kassem[1b], Ehsan Noroozinejad Farsangi[2c], Fadzli Mohamed Nazri[*1] and Eiki Yamaguchi[3d]

[1]*School of Civil Engineering, Universiti Sains Malaysia, Engineering Campus, 14300 Nibong Tebal, Penang, Malaysia*
[2]*Faculty of Civil and Surveying Engineering, Graduate University of Advanced Technology, Kerman, Iran*
[3]*Department of Civil Engineering Kyushu Institute of Technology Tobata, Kitakyushu 804-8550, Japan*

(*Received November 6, 2019, Revised December 23, 2019, Accepted January 4, 2020*)

Abstract. The use of passive energy dissipation devices has been widely used in the construction industry to minimize the probability of damage occurred under intense ground motion. In this study, collapse margin ratio (CMR) and fragility curves are the main parameters in the assessment to characterize the collapse safety of the structures. The assessment is done on three types of RC frame structures, incorporating three types of dampers, viscoelastic, friction, and BRB dampers. The Incremental dynamic analyses (IDA) were performed by simulating an array of 20 strong ground motion (SGM) records considering both far-field and near-field seismic scenarios that were followed by fragility curves. With respect to far-field ground motion records, the CMR values of the selected frames indicate to be higher and reachable to safety margin more than those under near-field ground motion records that introduce a high devastating impact on the structures compared to far-field excitations. This implies that the near field impact affects the ground movements at the site by attenuation the direction and causing high-frequency filtration. Besides that, the results show that the viscoelastic damper gives better performance for the structures in terms of reducing the damages compared to the other energy dissipation devices during earthquakes.

Keywords: collapse margin ratio; dampers; far-field; near-field; fragility curve; building resilience

1. Introduction

According to Marko *et al*. (2004), earthquakes are one of the biggest threats to life on this planet, by having devastated countless towns and villages. All these have led to different considerations towards structural safety, serviceability, and the potential of economic loss. Furthermore, those parameters are important to be considered in the structural design of the buildings under seismic loading. Hence, it is necessary to construct a structure considering the earthquake resistance at a specific intensity shaking (Juni P *et al*. 2017). In order to achieve a sustainable structural design with reduced economic loss, earthquake engineering requirements in building codes are used to prevent the collapse of buildings and to ensure the safety of building occupants during extreme ground motions. In recent years, the development and implementation of energy dissipating devices resulted in significantly reducing the seismic demand of the structure becomes popular among both researchers and practicing engineers.

The performance limit states are important parameters of Performance-Based Earthquake Engineering (PBEE) which can be defined through incremental dynamic analysis (IDA) curve (Vamvatsikos and Cornell 2002). Meanwhile, the IDA curve can be obtained when the structure undergoes incremental dynamic analysis (IDA) introduced into a few seismic records. From the outcome extracted from IDA, the fragility curve can be developed which represents the probability of the structural damage due to the earthquake events (Kammula *et al*. 2014).

There are so many various studies that have concentrated on exploring the seismic performance of the structure with implementing the passive energy dissipation devices which are also known as dampers (Khorami *et al*. 2017, Lavan 2015, Hoveidae *et al*. 2019, Montgomery and Christopoulos 2014, Alih *et al*. 2018, Xie 2005, Kim and Kim 2017, Yang *et al*. 2017, Cetin *et al*. 2017, Zhang *et al*. 2019, Losanno *et al*. 2017, Sun *et al*. 2019, Cetin *et al*. 2019, Hessabi *et al*. 2017, Casapulla 2015, Guan *et al*. 2018, Silwal *et al*. 2016, Manie *et al*. 2015). However, only a few studies have specialized in the assessment of the seismic performance considering different types of dampers using a probabilistic approach (Seo *et al*. 2014, Hamidia *et al*. 2014, Sani *et al*. 2017, Kitayama and Constantinou 2016). Other than that, from recent studies mentioned before, only Kitayama and Constantinou (2016) considered

∗Corresponding author, Associate Professor
E-mail: cefmn7@gmail.com
[a]M. Sc.
E-mail: puterinihal95@gmail.com
[b]Ph.D. Student
E-mail: engmmk93@gmail.com
[c]Assistant Professor
E-mail: noroozinejad@kgut.ac.ir
[d]Professor
E-mail: yamaguch@civil.kyutech.ac.jp

ISSN: 2092-7614 (Print), 2092-7622 (Online)

both seismic scenarios which are far-field and near-field ground motion records and the other studies only considered either far-field or near-field ground motion records. Furthermore, the use of dampers has been widely used in recent years and the use of collapse margin ratio is an important tool to evaluate the collapse safety for the structures with the use of several types of dampers. One main type of dampers is Friction dampers. The friction devices can provide rigidity and the desired energy dissipation capability (Kitayama and Constantinou 2016). According to Soong and Spencer Jr (2002), friction dampers used a solid friction mechanism that developed between two solid bodies sliding to another in order to produce the required energy dissipation. Meanwhile, studies by Zhu and Zhang (2008), stated that the friction damping devices dissipate the energy by the single friction mechanism built on the sliding layer, which is a relatively inexpensive and efficient approach to energy dissipation. The application of friction dampers results in a significant reduction of internal forces.

In addition to that, Viscoelastic dampers consist of viscoelastic materials used within structural systems, which are typically copolymers or glassy substances that dissipate energy by shear deformation. According to Tubaldi *et al*. (2015), the use of viscoelastic dampers has become increasingly common in the development and refurbishment of civil structures subjected to earthquake loads, as it often allows for the mitigation of undesirable features of structural reaction (Asano *et al*. 2000). As well, according to Xu *et al*. (2003), optimization analysis of structures with viscoelastic dampers includes the optimization of viscoelastic dampers parameters and locations in the structure are very important because the parameters and locations of viscoelastic dampers will lead to the most effective absorption. Moreover, viscoelastic damper comprises of flaky viscoelastic materials attached to steel plates and, if shear deformation occurred in viscoelastic materials, energy dissipation occurred due to dynamic loads (Zhang *et al*. 2019). Nevertheless, Symans *et al*. (2008) reported that viscoelastic dampers are used in structures to minimize structural vibration induced by many different types of dynamic loads. Finally, Kim and Choi (2004), studied the effect of viscoelastic dampers towards 5-storey and 25-storey rigid frame connected to braced frames. The parametric study shows that the viscoelastic dampers are able to minimize the dynamic responses of the structures by reducing the maximum displacement occurred. Furthermore, buckling restrained brace, BRB provides stiffness and energy dissipation throughout the height of the structure and present good hysteretic behavior. Other than that, BRB is vulnerable to residual displacements were functioning in reducing overall structural performance (Maley *et al*. 2010). In addition, Kim and Choi (2004), studied the seismic responses of structures with the use of BRBs and causes a reduction in maximum displacements of structures as the stiffness of BRBs increases and meanwhile, the wise distribution of the BRBs towards each storey results in a good structural performance especially in reducing the inter-story drift. Moreover, Xie (2005) conducted a study that represented a summary of BRB. Accordingly, when the brace is subjected to large compressive forces, it results in buckling deformation and present unsymmetrical hysteretic behavior in tension and compression. Ultimately, recent research suggested the technique of buildings with BRBs for low-intensity ground motion with regular occupancy showing adequate performance if it meets the Operational performance level suggests that the main framework and braces system should not lead to significant extensive damage. Based on the studies, the building shows adequate performance under Life Safety performance level and can be easily repaired which indicates when the main structural system remains to sustain at the elastic range and stay undamaged, the bracing device produces substantial plastic activity that allows a large amount of input energy to be dissipated. When the main structural system deforms further than the elastic range, the structural damage is concentrated in the braces' structure (Terán-Gilmore *et al*. 2015, Teran-Gilmore and Virto 2009).

One of the main objectives of the seismic design philosophy is to design structures so that under intense ground motions the structural collapse is prevented. Therefore, the safety margin against structural collapse must be quantified (Deierlein *et al*. 2007). Hamidia *et al*. (2014), recently proposed a technique for predicting the side-sways margin collapse ratio of buildings using linear viscous dampers as described by the FEMA P695 methodology. The proposed technique is defined as much simpler because the FEMA P695 methodology needs only median sideways collapse capability as compared to the whole collapse fragility curve. Moreover, the determination of the structure's collapse margin ratio is affected by many factors such as pre-collapse elongation of the structural fundamental period, earthquake strength estimation, seismic risk potential, and spectral shape disparity between the ground motion medium spectrum and the design spectrum (Ou *et al*. 2014, Kassem *et al*. 2019). Other than that Tohidian and Manafpour (2015) also studied the collapse margin ratio for reinforced concrete moment resisting frames of 3-storey, 6-storey and 10-storey by considering different types of soil classifications and ductility levels. The collapse is assessed for each of the ground motion records and the median value collapse, SCT is calculated. Last but not least Seo *et al*. (2014), used the collapse margin ratio to evaluate the seismic performance of steel moment-resisting frames (MRFs) with the incorporation of fluid viscous dampers. He *et al*. (2018) stated a collapse margin ratio is one of the quantified indexes for structural collapse resistance to evaluate the efficiency of introducing BRBs in earthquake-resistant reinforced concrete frames. Eventually, the aim of this research is to develop the fragility curves of RC-MRFs with and without dampers subjected to different seismic scenarios, as well as to evaluate the collapse margin ratio (CMR) subjected to different types of dampers. Hence, this research focuses on the assessment of the structure with the use of dampers considering near-field (NF) and far-field (FF) seismic scenarios through the CMR, which can be defined by the fragility curves of the investigated dampers; viscoelastic, friction and BRB.

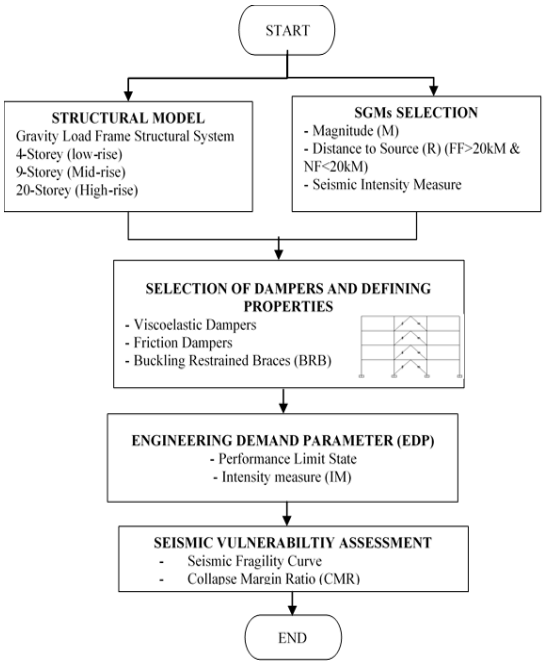

Fig. 1 Flowchart of the study work for assessing dampers effect due to seismic scenarios

2. Utilized methodology

In this work, the assessment related to collapse margin resistance of gravity load designed structures are investigated by intervening different type of dampers through (4-storey, 9-storey and 20-storey) buildings due to seismic scenarios. The structural models represent three types of clusters as low-rise, mid-rise, and high-rise buildings that were simulated, and analyzed using a nonlinear platform. A nonlinear dynamic analysis approach is adopted to assess the structural vulnerability of the structures with and without intervention of the damper systems, which are known as a key tool to determine the safety margin of the structure. These analyses were performed by conducting 20 seismic records as a series of nonlinear time history (NL-TH) divided by near-field (NF) and far-field (FF) SGMs. The ground motion records were selected based on the magnitude and distance to source as a criterion for this study. In addition to that, seismic fragility curves were developed to evaluate the seismic performance of structural models according to 4-performance limit sates (OP: Operational Performance, IO: Immediate Occupancy, LS: Life Safety, and CP: Collapse Prevention). Eventually, the collapse margin ratios (CMRs) as a seismic indicator have been calculated after performing the fragility analyses of Collapse level at 50% probability of damages as referred to FEMA P-695 process. Fig. 1 shows and describes the methodology of this study.

2.1 Structural model configurations

The investigated structures are 4-storey, 9-storey and 20-storey with total height 12 m, 27 m, and 60 m respectively. Each frame consists of three bays with 6 m width each and has a similar storey height which is 3 m. Fig. 2 shows the investigated structural models. The frames are analyzed and designed according to Eurocode 2. Several properties are assumed for each of the frames. The material type used is concrete with concrete grade C30. Concrete compressive strength, $f'c$ and weight per unit volume are 30 MPa and 24 kN/m^3 respectively. Meanwhile the modulus of elasticity of concrete, E is 25,743 MPa. The yield stress of reinforced steel, f_y is 460 MPa. In this work, the concept of the strong column-weak beam is applied in designing the frames according to (Wongpakdee and Leelataviwat 2017)

Tables 1 and 2 show the details on the design assumptions of beam and column specifications with reinforcement detailing of each, respectively. Fig.3 shows the detailing rebars of the columns designed. Each of the frame models undergoes clarification under gravity load cases in order to verify whether the sizes of properties assigned to the models is capable enough under gravity loads (dead load and live load) such as if there are any of the elements of the structure undergoes any overstress. All the frame models are stable under gravity loads and not exhibit any overstress at the reinforcement assigned to the elements of the structure to provide lateral resistance to withstand earthquake loading in seismic regions. Friction damper and viscoelastic damper are defined in terms of link elements. The mass of the dampers is defined according to the size of the dampers, meanwhile, in terms of force capacity of the dampers, different values of forces can be used for different types of buildings. However, the force capacities for each damper were defined uniformly for all the frames. Meanwhile, for buckling restrained braced are defined in terms of the size of the core segment of the brace and tension and compression limit.

2.2 Properties of dampers

In this study, there are three types of passive dampers which are friction damper, viscoelastic damper and buckling restrained brace (BRB). Configuration of dampers in this study is in the form of chevron configuration or known as inverted- V because of the effectiveness and economic issues to provide lateral resistance to withstand earthquake loading in seismic regions. Friction damper and viscoelastic damper are defined in terms of link elements. The mass of the dampers is defined according to the size of the dampers, meanwhile, in terms of force capacity of the dampers, different values of forces can be used for different types of buildings. However, the force capacities for each damper were defined uniformly for all the frames. Meanwhile, for buckling restrained braced are defined in terms of the size of the core segment of the brace and tension and compression limit.

In terms of damping coefficient, even though the lower values of the damping coefficient are often used, the value of 5% damping is selected to match the requirements of Eurocode 8 horizontal response spectrum and to be consistent with several previous studies (Costanzo *et al*. 2018, Karamanci and Lignos 2014, Symans *et al*. 2008).

Hence, in this study, the damping coefficient is assumed to be 5%. Fig. 4 shows the dampers' placement in the frame structures.

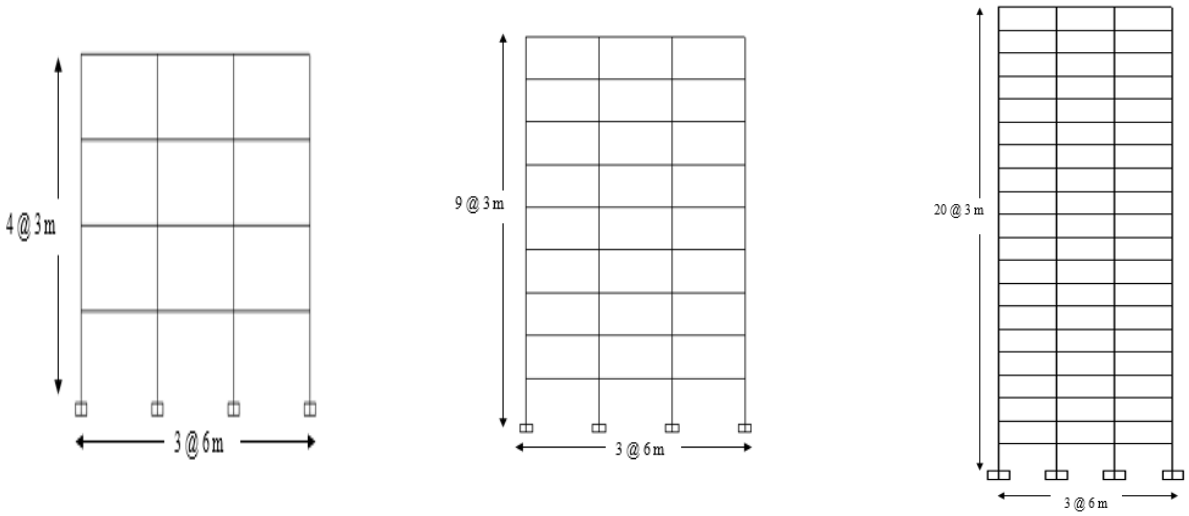

(a) (b) (c)

Fig. 2 Elevation view of the frame buildings: a) 4-storey b) 9-storey c) 20-storey

Table 1 Beam sizes and reinforcement details

No. of storey	Sizes (mm × mm)	Reinforcement (mm^2)	Shear Link	Beam Reinforcement Details
4	300 × 600	6H16 (1207)	8 mm links at 300 mm c/c	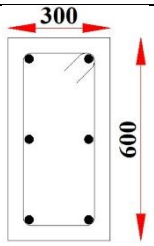
9	300 × 600	6H16 (1207)	8 mm links at 300 mm c/c	
20	300 × 600	6H16 (1207)	8 mm links at 300 mm c/c	

Table 2 Column sizes and reinforcement details

No. of storey	Sizes (mm × mm)	Reinforcement (mm^2)
4	400 × 400	8H16 (1610)
9	450 × 450	10H16 (2010)
	700 × 700 (1^{st} – 10^{th} story)	14H16 (2815)
20	500 × 500 (11^{th} – 14^{th} story)	8H16 (1610)
	450× 450 (15^{th} – 20^{th} story)	8H16(1610)

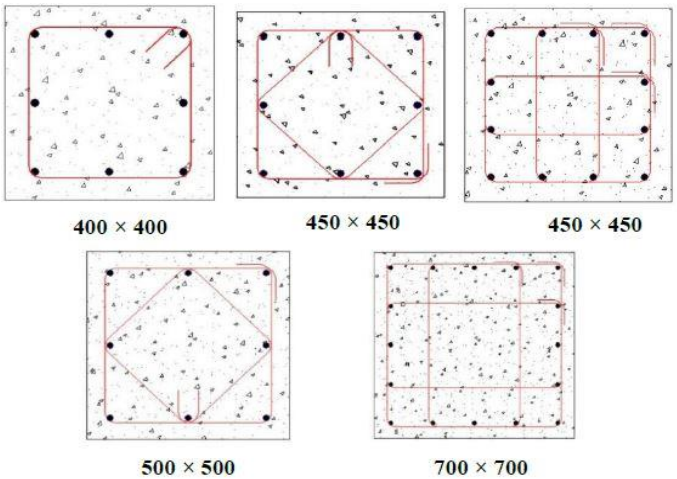

Fig. 3 Column sizes and reinforcement details

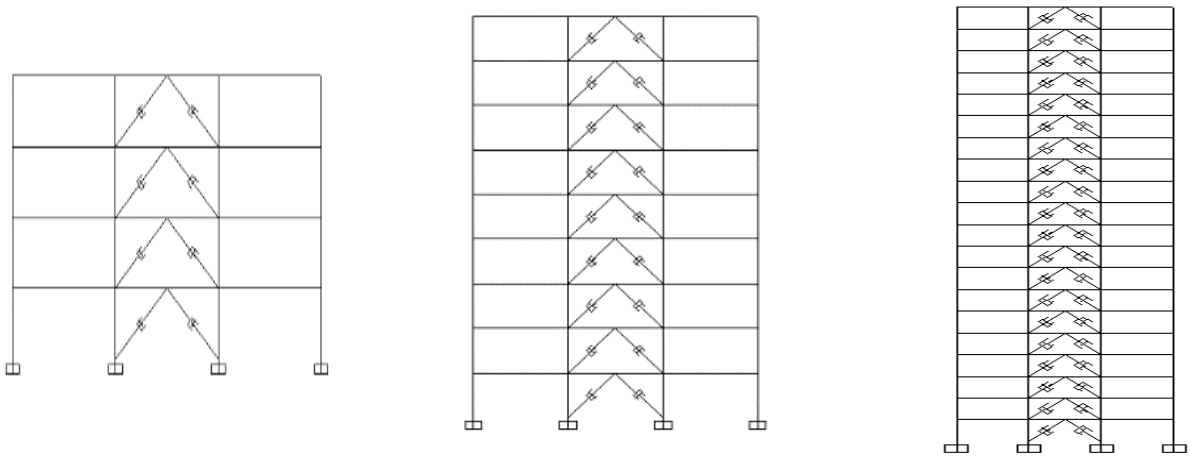

(a) (b) (c)

Fig. 4 Dampers placement for: (a) 4-storey (b) 9-storey (c) 20-storey

Table 3 Near-Field NF ground motion records

No	Earthquake	Date	Magnitude, Mw	Epicentral Distance, km	PGA(g)
1	Anza (Horse Canyon)-01	25/02/1980	5.19	5.85	0.275
2	Dursunbey, Turkey	18/07/1979	5.34	5.57	0.185
3	Fruili Italy-03	11/09/1976	5.50	16.26	0.366
4	Helena Montana-01	31/10/1935	6.00	2.07	0.614
5	Imperial Valley-07	15/10/1979	5.01	10.83	0.204
6	Izmir Turkey	16/12/1977	5.30	0.74	0.391
7	Lytle Creek	12/09/1970	5.33	17.40	0.526
8	California	10/01/1987	6.10	14.60	0.223
9	Northwest China-03	11/04/1997	6.10	9.98	0.446
10	Parkfield-02 CA	28/09/2004	6.00	2.35	0.263

2.2.1 Friction dmper

Friction dampers were modelled as nonlinear link elements. The mass and force capacity of the friction dampers were defined as 240 kg and 1000 kN, respectively. The friction dampers are assigned to the models using two joint links.

2.2.2 Viscoelastic damper

Viscoelastic dampers were modeled as fixed viscoelastic damper using linear type. The mass and force capacity of viscoelastic dampers were defined as 254 kg and 1000 kN, respectively based on Qamaruddin (2017). The viscoelastic dampers are assigned to the models using two joint links.

2.2.3 Buckling rstrained baces (BRBs)

BRBs were modeled as steel bracing. The tensile yield stress of BRB material is considered as 345 MPa. Modulus of elasticity of steel, E for BRBs is considered as 200 GPa. The core area of BRBs considered to be 3548.38 mm^2. Other than that, the axial resistance based on (Ghowsi and Sahoo 2013), consists of tension and compression limitation on used for the BRBs are 1223.3 kN and 1345.6 kN respectively. The leaning column is limited in terms of the connection between columns and BRBs in order to have the same lateral displacement at each floor level as the adjacent braced frame column. This can be accomplished through the use of rigid link beams with fixed ends between the BRBs and the leaning columns at each floor level.

Hence, in the present study, the pinned connection is used between the columns and BRBs.

2.3 Strong ground motions selection

In this study, there are two parameters that are taken into consideration in the selection procedure of the SGMs, which are the event magnitude and distance from the site to source. The earthquake scenarios are selected with the range magnitude between 5.0 to 7.0 with different distance from site to source.

According to Alwaeli *et al*. (Alwaeli *et al*. 2017), the distance between site to the source generally influences the ground motion at the site through path attenuation and high-frequency filtration. The seismic wave is either amplified or dissipated depends on the characteristics of the soil strata while traveling from the bedrock to the ground motion. The classification distance from the site to source for the far-field and near-field is not exactly clarified. Some of the researchers suggested considering the distance from site to the source less than 20km for near-field case meanwhile, greater than 20km considered as the far-field case.

Other than that, stated by FEMA P695 (2009), far-field record set is a distance from sites located greater than or equal to 10 km from fault rupture and meanwhile, the near-field record set is a distance from sites less than 10 km from the fault rupture. Hence, in this study, near-field ground motion is considered as the distance from site to source less

Table 4 Far-Field (FF) ground motion records

No	Earthquake	Date	Magnitude, Mw	Epicentral Distance, km	PGA(g)
1	Georgia USSR	15/06/1991	6.20	63.53	0.321
2	Imperial Valley-01	06/06/1938	5.00	32.44	0.453
3	N. Palm Springs	08/07/1986	6.06	54.67	0.328
4	Northern Calif-06	18/12/1967	5.20	37.11	0.573
5	Northridge-01	17/01/1994	6.69	35.66	0.158
6	Parkfield	28/06/1966	6.19	63.34	0.210
7	Sabah	05/06/2015	6.00	20	0.125
8	Roermond Netherlands	13/04/1992	5.30	55.48	0.427
9	Taiwan SMART1(40)	20/05/1986	6.32	58.69	0.295
10	Whittier Narrows-01	01/10/1987	5.99	72.62	0.456

Table 5 Performance limit % drift of the structures (Vision 2000)

Performance Level		OP	IO	LS	CP
Maximum % of ISDR		0.5%	1.0%	1.5%	2.5%
Allowable Maximum Displacement (m)	4-storey	0.06	0.12	0.18	0.30
	9-storey	0.14	0.27	0.40	0.68
	20-storey	0.30	0.60	0.90	1.50

than or equal to 20 km meanwhile, far-field ground motion is considered as the distance from site to source greater than 20 km. Other than that, several seismic codes recommend that the nonlinear dynamic analysis must be performed with a minimum of three to seven sets of ground motions such as FEMA 356, UBC97, IBC2006 and NEHRP.

In this study, two sets of 10 natural earthquake records each with a total of 20 records were presented considering both seismic scenarios which are near-field and far-field earthquakes. The Pacific Earthquake Research Centre database (PEER) has been used to select the SGM records. Tables 3 and 4 show the specifications of the near-field (NF) and far-field (FF) ground motion records respectively.

2.4 Seismic vulnerability assessment

2.4.1 Fragility estimation

The seismic fragility curve is one of the most important essential elements in the assessment of damage from earthquake events. The fragility curves represent the probabilities of structural damage due to earthquake events as a function of ground motion intensities such as peak ground motion acceleration (PGA), spectral acceleration (Sa) and spectral displacement (Sd). The fragility curves vary with the type of structural systems, characterization of earthquakes excitation and performance levels chosen (Kammula *et al*. 2013). In order to extract the occurrence probability of limit states from IDAs output, the fragility curves would be used. The occurrence probabilities of limit states were calculated with cumulative density function (CDF) and delineated with IM in fragility curves (Sani *et al*. 2015, 2017).

Meanwhile, in order to develop fragility curves, the selection of the seismic parameters such as spectral acceleration (Sa), spectral displacement (Sd), peak ground velocity (PGV) and peak ground acceleration (PGA) need to be chosen. Since in this study, the spectral acceleration, Sa(T1) is the parameter used to develop the IDA curves, hence, the spectral acceleration, Sa(T1) is selected to be the corresponding parameter in developing the fragility curves. According to Shinozuka *et al*. (2003), the cumulative distribution functions are calculated by dividing the number of data points that reached a particular damage state by the number of points of the whole sample. The equation needed to develop the fragility curves is shown in Eq. (1) mentioned in (Ibrahim and El-Shami 2000).

$$P\left[\frac{D}{Sa[T1]}\right]=\phi\left(\frac{Ln\left(Sa[T1]\right)-\mu}{\sigma}\right) \quad (1)$$

Where ϕ is the standard normal cumulative distribution function, μ and σ are the mean and standard deviation of the logarithm Sa at the damage state, and D specified as the mentioned performance level (Ibrahim and El-shami 2011). Besides, to measure the performance of the structures, the percentage of drifts will be used to observe the maximum displacement occurred to the structures that lead to the structural collapse as illustrated in Table 5.

2.4.2 Collapse margin ratio (CMR)

Defined by FEMA P695, the ratio between the median collapse intensity obtained from the fragility curve and Maximum Considered Event (MCE) intensity called, as collapse margin ratio (CMR) is the critical parameter in the evaluation to describe the stability of the structure collapse. In the assessment of the seismic performance of the structures incorporation different types of dampers, the FEMA P695 suggests the need to apply a collapse assessment methodology to structures with the use of damping systems. The collapse Margin Ratio (CMR) can be determined with the use of series ground motion records and collapse data obtained from IDA and fragility analyses. The CMR can be defined through fragility curves, which represent the probability of structural damage with the specific percentage drift based on performance limit states.

The FEMA P695 recommends to determine the seismic collapse safety margin of structures based on a probabilistic indicator called collapse margin ratio (CMR) defined as the ratio of the amount of intensity measure (IM) increased to

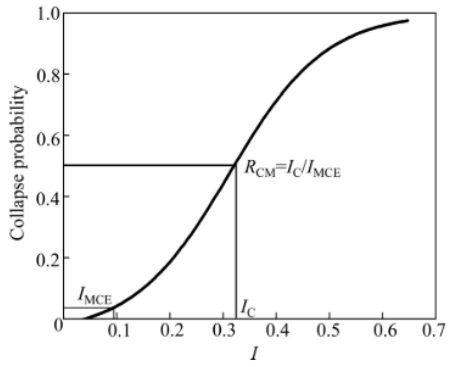

Fig. 5 CMR indicator from a collapse fragility curve (Ou *et al*. 2014)

achieve building collapse by 50% of the ground motion to the intensity measure (IM) of the maximum considered earthquake (MCE) as shown in Eq. (2).

$$CMR = \left[\frac{IM_{\%50\ Collapse}}{IM_{MCE}} \right] \quad (2)$$

According to Malaysia National Annex (2017) the value of PGA for Peninsular Malaysia is between 0.02 g to 0.10g for 500 years return period. Meanwhile, the value of PGA for Sabah and Sarawak is between 0.06 g to 0.12 g with the same return period. Accordingly, 3 values of PGA were selected as a reference of peak ground acceleration, agR which are 0.02 g, 0.06 g, and 0.12 g to overcome a wide range of PGA in Malaysia. In this case, considering the most critical value of PGA occurred in East Malaysia which is 0.12 g, the value of peak ground acceleration (PGA) for MCE is taken as 0.16g (0.424 g for Sa(T1)). Where Fig.5 shows an example of a fragility curve obtained from the Eq. 2. Ic is the earthquake intensity at 50% from the probability of structural collapse which occurred at the CP state. CMR indicates the ratio of *Ic* to the earthquake intensity corresponding to MCE, IMCE.

3. Results and discussion

3.1 Fragility curves

In this study, the assessment has been done by using two sets of ground motion records representing far-field (FF) and near-field (NF) seismic scenarios. he seismic intensity measure (IM) used in this study is spectral acceleration, Sa(T1). Each frame is subjected to the ground motion records until it reaches the collapse state (CP) at 2.5%. The fragility curves were developed based on four performance limit states which are Operational Performance (OP), Immediate Occupancy (IO), Life Safety (LS) and Collapse Prevention (CP) defined as 0.5%, 1.0%, 1.5%, and 2.5% drift respectively. In order to develop the fragility curves, there are two important parameters which are mean and standard deviation. The parameters are calculated for all the frames subjected to ten ground motion records for each of the seismic scenarios consists of far-field records and near-field ground motion records based on the equation proposed by Ibrahim and El-Shami (Ibrahim and El-Shami 2011).

After calculating the mean and standard deviation for all cases and frames, the fragility curves were developed as the parameter that estimates the probability of the damage. The fragility curves consist of three parts which are the results for 4-storey, 9-storey and 20-storey frames. The comparison for each part consists of the performance of the frames without dampers and frames with the use of dampers subjected to seismic scenarios.

3.1.1 4-Storey fragility curve

Based on the fragility analysis for 4-storey frame without dampers and with the use of friction damper, viscoelastic damper, and BRB. The analysis results were illustrated to compare the probability of damages under the influence of far-field (FF) and near field (NF) SGM records at spectral acceleration Sa(T1) equals to 1.0 g regarding different types of dampers as shown in the Fig. 6 and Table 6.

For far-field records, it shows that 4-storey frame without dampers causes 100% damage of the structures higher than the 4-storey frame with the use of dampers with less than 100% damage of the structures. The probability of damage for 4-storey frame with the use of friction damper causes of 80% damage of structures higher than the frame with the use of viscoelastic damper and BRB causes of 50% damage of structures, respectively.

Meanwhile, comparing with near-field records it shows that 4-storey frame without dampers causes 100% damage of the structures higher than the 4-storey frame with the use of dampers with less than 100% damage of the structures except for frame with the use of friction damper. The probability of damage for 4-storey frame with the use of friction damper causes 100% damage of structures the same as the frame without the use of dampers and higher than compared to the BRB and viscoelastic damper causes 80% and 50% damage of the structures, respectively.

For both seismic scenarios, the friction damper shows a quite high probability of damage, still with the use of damper shows some improvement in structures behavior when subjected to the earthquake which can be seen using BRB and viscoelastic damper. From this comparison, this clearly shows that passive energy dissipation devices which are friction damper, viscoelastic damper and BRB give a better performance of the structures in terms of damage of structures compared to the structures without the use of passive energy dissipation devices during the occurrence of the earthquakes.

3.1.2 9-storey fragility curve

Based on the fragility analysis for 9-storey frame without dampers and with the use of friction damper, viscoelastic damper, and BRB. The analysis is illustrated to compare the probability of damages under the effect of far-field (FF) and near field (NF) ground motion record at spectral acceleration Sa[T1] equals to 1.0 g regarding different types of dampers as shown in the Fig. 7 and Table 7.

For far-field records, it shows that the 9-storey frame

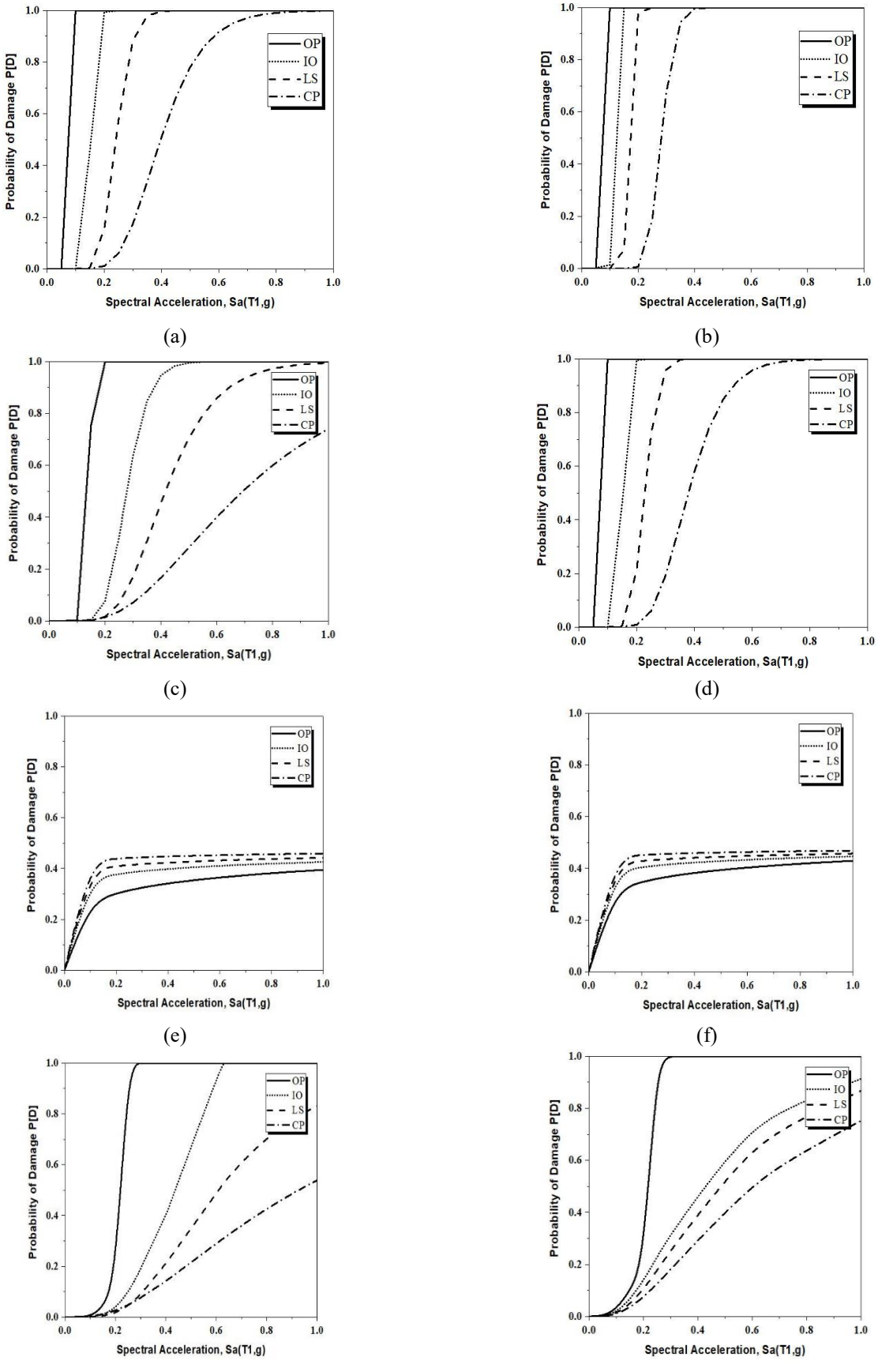

Fig. 6 Fragility curves for 4-storey frame (a): Without dampers (FF) (b): Without dampers (NF) (c): Friction damper (FF) (d): Friction damper (NF) (e): Viscoelastic damper (FF) (f): Viscoelastic damper (NF) (g): BRB (FF), (h): BRB (NF)

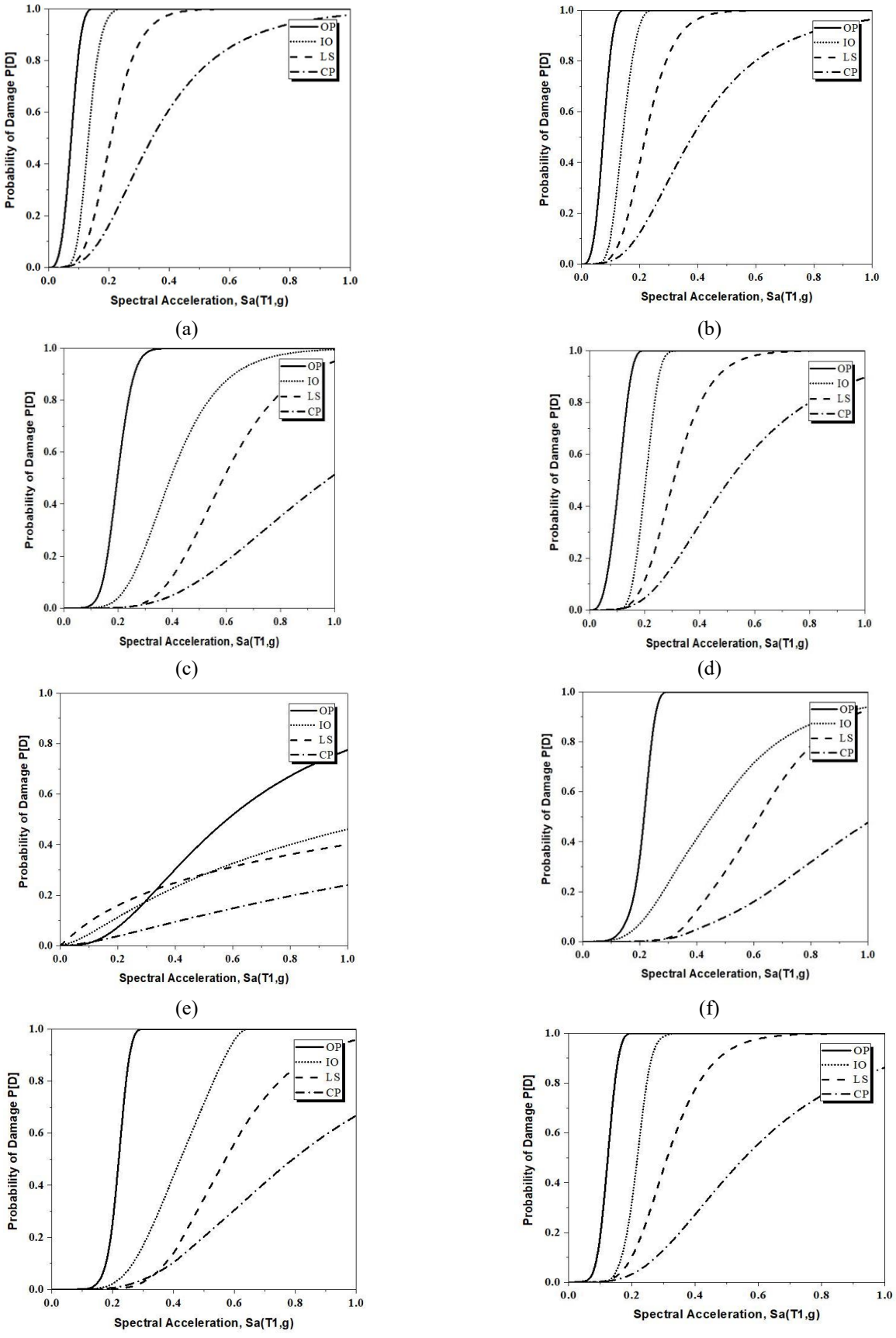

Fig. 7 Fragility curves for 9-storey frame (a): Without dampers (FF) (b): Without dampers (NF) (c): Friction damper (FF) (d): Friction damper (NF) (e): Viscoelastic damper (FF) (f): Viscoelastic damper (NF) (g): BRB (FF) (h): BRB (NF)

Table 6 Probability of damage at CP state for 4-storey at 1.0 g

Probability of damage (%) at CP state		
Models/ Seismic Scenario	Far-Field	Near-Field
Without damper	100 %	100 %
Friction damper	80 %	100 %
Viscoelastic damper	50 %	50 %
BRB	50 %	80 %

Table 7 Probability of damage at CP state for 9-storey at 1.0 g SA[T1]

Probability of damage (%) at CP state		
Models/ Seismic Scenario	Far-Field	Near-Field
Without damper	100 %	100 %
Friction damper	50 %	90 %
Viscoelastic damper	24%	50 %
BRB	70 %	90 %

Table 8 Probability of damage at CP state for 20-storey at 1.0g Sa[T1]

Probability of damage (%) at CP state		
Models/ Seismic Scenario	Far-Field	Near-Field
Without damper	60 %	80 %
Friction damper	41%	40 %
Viscoelastic damper	20 %	60 %
BRB	20 %	70 %

without dampers causes 100% damage of the structures higher than the 9-storey frame with the use of dampers with less than 100% damage of the structures. The probability of damage for 9-storey frame with the use of dampers results with the use of BRB causes 70% damage of structures higher than with the use of friction damper and viscoelastic damper causes only 50% and 24% damage of structures, respectively.

Meanwhile, comparison under near-field records shows that 9-storey frame without dampers causes 100% damage of the structures higher than the 9-storey frame with the use of dampers with less than 100% damage of the structures. The probability of damage for 9-storey frame with the use of dampers results with the use of friction damper and BRB causes 90% damage of structures higher compared to the viscoelastic damper only causes 50% damage of the structures.

For both seismic scenarios, shows that 9-storey frame with the use of dampers gives a better performance of the structures compared to the 9-storey frame without the use of dampers. From both seismic scenarios, viscoelastic damper causes a lower percentage of damage compared to the friction damper and BRB but, still shows very effective improvement in structures behavior when subjected to the earthquake. From this comparison, this clearly shows that passive energy dissipation devices which are friction damper, viscoelastic damper and BRB give a better performance of the structures in terms of damage of structures compared to the structures without the use of passive energy dissipation devices during the occurrence of the earthquakes.

3.1.3 20-storey fragility curve

Based on the fragility analysis for 20-storey frame without dampers and with the use of friction damper, viscoelastic damper, and BRB. The analysis results are illustrated to compare the probability of damages under the effect of far-field (FF) and near field (NF) ground motion record at spectral acceleration Sa[T1] equals to 1.0 g regarding different types of dampers as shown in the Fig. 8 and Table 8.

For far-field records, it shows that the 20-storey frame without dampers causes 60% damage of the structures higher than the 20-storey frame with the use of dampers with less than 60% damage of the structures. The probability of damage for 20-storey frame with the use of dampers results with the use of viscoelastic damper and BRB causes only 20% damage of structures higher than with the use of friction damper which only causes 41% damage of structures.

Meanwhile, comparison under near-field records shows that 20-storey frame without dampers causes 80% damage of the structures higher than the 20-storey frame with the use of dampers with less than 80% damage of the structures. The probability of damage for 20-storey frame with the use of BRB causes 70% damage of structures higher than viscoelastic damper and friction damper which causes 60% and 40% damage of structures respectively.

Both seismic scenarios show that for 20-storey frame with the use of dampers gives a better performance of the structures compared 20-storey frame without the use of dampers. From both seismic scenarios, viscoelastic damper causes the lower probability of damage compared to the friction damper and BRB but, still shows very effective improvement in structures behavior when subjected to the earthquake. From this comparison, this clearly shows that passive energy dissipation devices which are friction damper, viscoelastic damper and BRB gives better performance of the structures in terms of damage of structures compared to the structures without the use of passive energy dissipation devices during the occurrence of the earthquakes.

3.2 Collapse Margin Ratio (CMR)

The CMR suggested by FEMA P695 is one of the best collapse indicators that has been developed over the past decades. This indicator would describe the structure's collapse safety by combining the median spectral acceleration and MCE spectral acceleration in the fundamental period of the site classification structure in Malaysia-East Asia. The median intensity of collapse is specified once half of the structure has the type of life-threatening failure or the possibility of damage is exceeded (Pcollapse=50%). In this study, by taking the spectral acceleration, Sa[T1] at 50% of CP state divide by the maximum considered earthquake (IMCE) which is taken as 0.424 g as Sa, which is equal to 0.16 g PGA based on the East Malaysia seismic zone stated in Malaysia National Annex 2017.

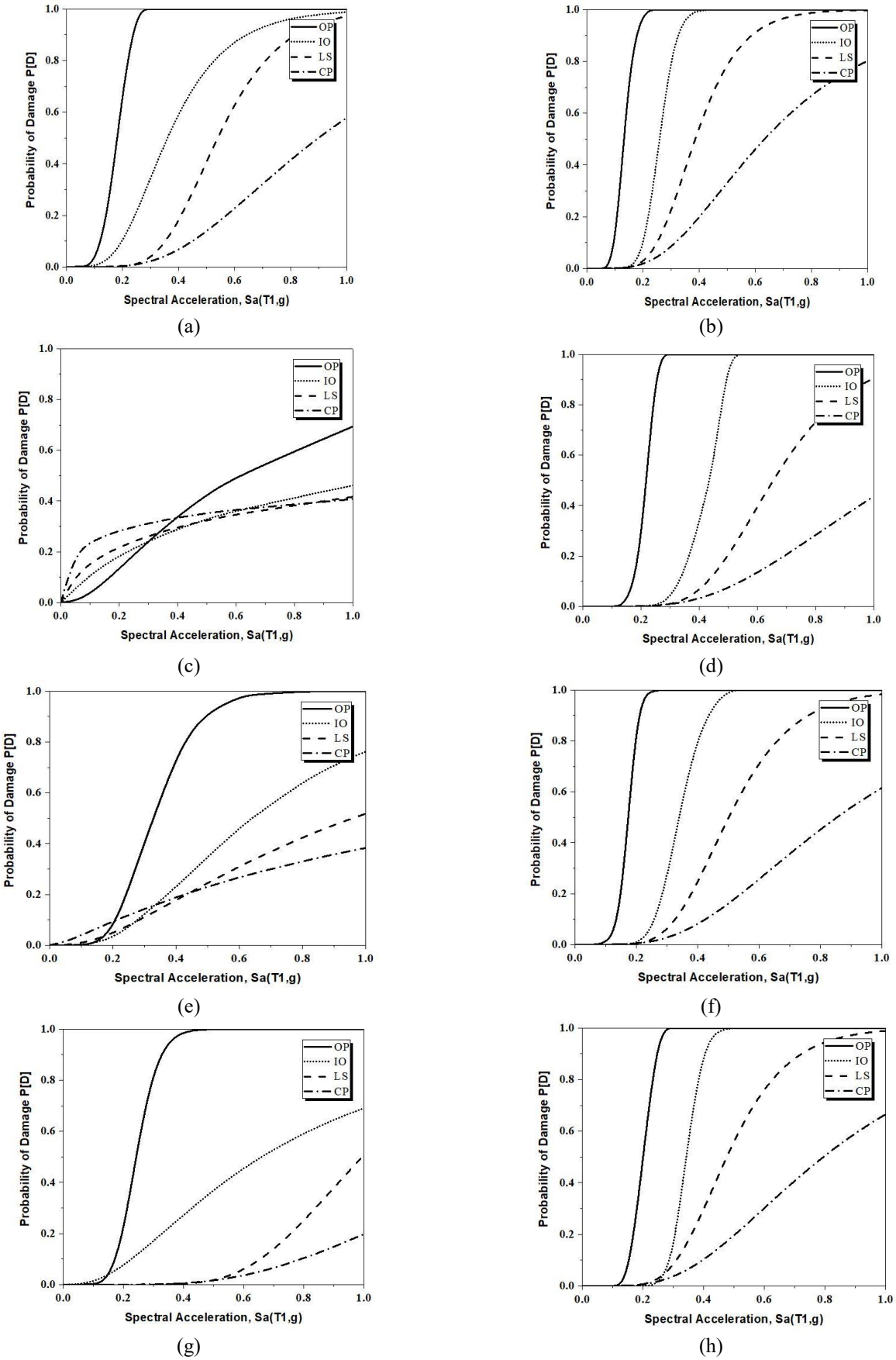

Fig. 8 Fragility curves for 20-storey frame (a): Without dampers (FF) (b): Without dampers (NF) (c): Friction damper (FF) (d): Friction damper (NF) (e): Viscoelastic damper (FF) (f): Viscoelastic damper (NF) (g): BRB (FF), (h): BRB (NF)

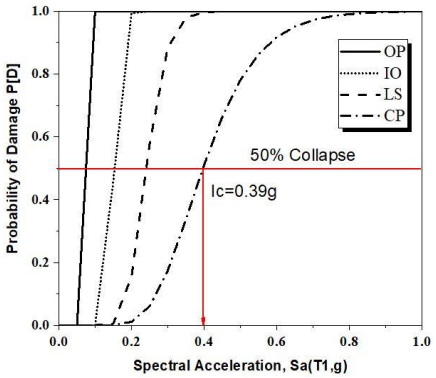

(a)

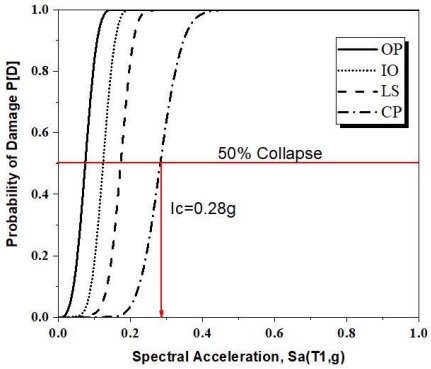

(b)

Fig. 9(a) Collapse fragility curve for (FF) ground motion records without dampers (b) Collapse fragility curve for (NF) ground motion records without dampers

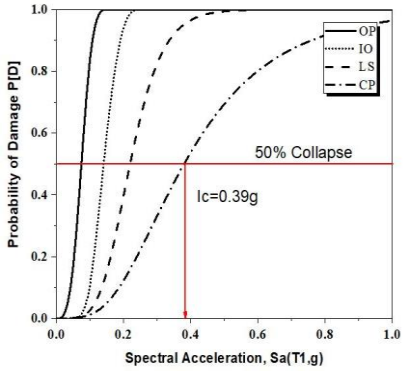

(a)

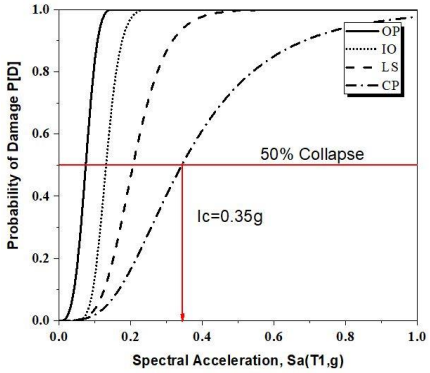

(b)

Fig. 10(a) Collapse fragility curve for (FF) ground motion records without dampers (b) Collapse fragility curve for (NF) ground motion records without dampers

Table 9 Collapse margin ratios (CMR) for 4-storey

Seismic Scenario	4-storey frame	$Ic_{50\%\ collapse}$ (g)	I_{MCE} (g)	CMR
Far-field	Without damper	0.39	0.424	0.91
	Friction damper	0.69	0.424	1.63
	Viscoelastic damper	2.02	0.424	4.76
	BRB	0.93	0.424	1.87
Near-field	Without damper	0.28	0.424	2.19
	Friction damper	0.38	0.424	0.89
	Viscoelastic damper	1.06	0.424	2.50
	BRB	0.68	0.424	1.60

Table 10 Collapse margin rations (CMR) for 9-storey

Seismic Scenario	9-storey frame	$Ic_{50\%\ collapse}$ (g)	I_{MCE} (g)	CMR
Far-field	Without damper	0.39	0.424	0.90
	Friction damper	0.98	0.424	2.31
	Viscoelastic damper	2.88	0.424	6.79
	BRB	0.79	0.424	1.87
Near-field	Without damper	0.35	0.424	0.81
	Friction damper	0.51	0.424	1.20
	Viscoelastic damper	1.03	0.424	2.43
	BRB	0.56	0.424	1.31

3.2.1 CMR for 4-story frame

As an example, based on the collapse fragility curve in Fig. 9(a) and 9(b) which shows the spectral acceleration, Sa[T1] at 50% at CP state are taken from the fragility curves for 9-storey frame without damper under far-field and near-field records respectively. As well the Ic represents the spectral acceleration at 50% at CP state. Table 9 shows the CMR values for 4-storeys with and without dampers.

3.2.2 CMR for 9-story frame

As an example, based on the collapse fragility curve in Figs. 10(a) and 10(b) which shows the spectral acceleration, Sa[T1] at 50% at CP state are taken from the fragility curves for 9-storey frame without damper under far-field and near-field records respectively. As well the Ic represents the spectral acceleration at 50% at CP state. Table 10 shows the CMR values for 9-storeys with and without dampers.

3.2.3 CMR for 20-story frame

As another example based on the collapse fragility curve in Figs. 11(a) and 11(b) which shows the spectral acceleration, Sa[T1] at 50% at CP state are taken from the fragility curves for 20-storey frame without damper under far-field and near-field records respectively. Nevertheless, Figs.12 (a) and 12(b) shows the CMR for the following cases “friction damper”, “viscoelastic damper” and “BRB” for 20-storey frame. As well the Ic represents the spectral acceleration at 50% at CP state. Table 11 shows the CMR values for 20-storeys with and without dampers.

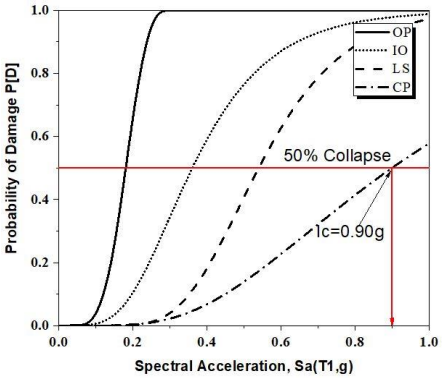

(a)

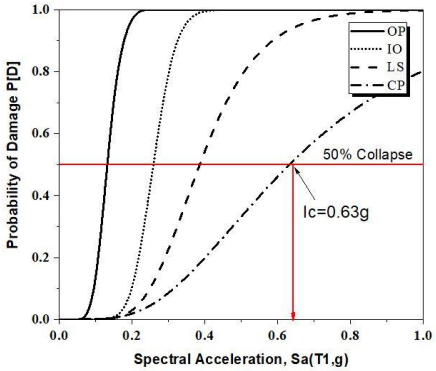

(b)

Fig. 11(a): Collapse fragility curve for (FF) ground motion records without dampers (b) Collapse fragility curve for (NF) ground motion records without dampers

Table 11 Collapse margin ratios (CMR) for 20-storey frame

Seismic Scenario	9-storey frame	$Ic_{50\%\ collapse}$ (g)	I_{MCE} (g)	CMR
Far-field	Without damper	0.90	0.424	2.12
	Friction damper	3.00	0.424	7.13
	Viscoelastic damper	1.60	0.424	3.77
	BRB	1.59	0.424	3.73
Near-field	Without damper	0.63	0.424	1.49
	Friction damper	1.09	0.424	2.57
	Viscoelastic damper	1.05	0.424	2.00
	BRB	0.79	0.424	1.87

4. Conclusion

This study evaluates the 4-storey, 9-storey and 20-storey RC buildings with the use of different types of dampers which are friction damper, viscoelastic damper, and BRB under far-field and near-field seismic scenarios. In this research, the nonlinear incremental dynamic analyses were performed to evaluate the structural performance of the structures with and without the use of dampers. The conclusions that can be drawn are:

• From the fragility curves, 4-storey, 9-storey and 20-storey frames with the use of dampers show a decrement in the percentage of damage of the structures when subjected to the strong ground motions. The most effective damper, when subjected to the ground motions considering both seismic scenarios which are far-field and near-field ground motion records, for the 4-storey and 9-storey frames, has been the viscoelastic damper, while for 20-storey frame the friction damper has shown the best performance. This clearly shows that the passive energy dissipation devices used in this study which are friction damper, viscoelastic damper and BRB gives a better performance of the structures in terms of reduction of the damage to the structures compared to the structures without the use of passive energy dissipation devices during the occurrence of the earthquakes.

• In this study, the CMR as the performance indicator of the structures with the use of dampers under both seismic scenarios has been defined from the fragility curves. Based on both seismic scenarios, the CMR values for the frames under far-field ground motion records are higher compared to the frames under near-field ground motion records. This indicates that the near field effect affects the ground motion at the site through path attenuation and induced high-frequency filtration. Meanwhile, for far-field ground motion records, the seismic wave can be dissipated into the soil while traveling from the bedrock to the ground level but still depends on the characteristics of the soil.

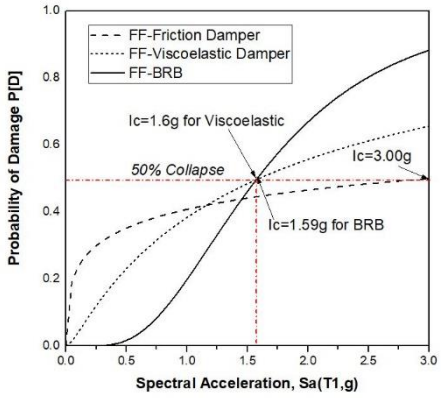

(a)

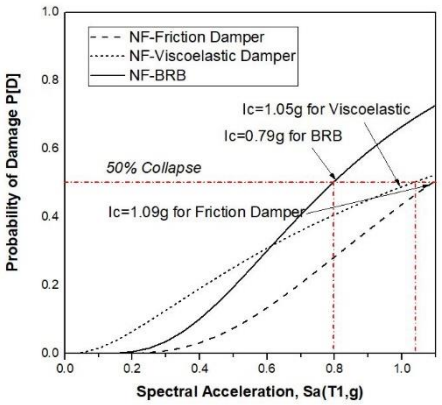

(b)

Fig. 12(a) Collapse fragility curve for (FF) ground motion records with dampers (b) Collapse fragility curve for (NF) ground motion records with dampers

Acknowledgment

This study is financially supported by Universiti Sains Malaysia, under the Research University Individual (RUI) Grant Scheme (8014080).

References

Agency, F.E.M. (2000), "Prestandard and commentary for the seismic rehabilitation of buildings", *Am. Soc. Civil Eng*. (ASCE).

Alwaeli, W., Mwafy, A., Pilakoutas, K. and Guadagnini, M. (2017), "A methodology for defining seismic scenario-structure-based limit state criteria for rc high-rise wall buildings using net drift", *Earthq. Eng. Struct. Dyn*., **46**(8), 1325-1344. https://doi.org/10.1002/eqe.2858.

Alih, S.C., Vafaei, M., Ismail, N. and Pabarja, A. (2018), "Experimental study on a new damping device for mitigation of structural vibrations under harmonic excitation", *Earthq. Struct*., **14**(6), 567-576. https://doi.org/10.12989/eas.2018.14.6.567.

Asano, M., Masahiko, H. and Yamamoto M. (2000), "The experimental study on viscoelastic material dampers and the formulation of analytical model", *Proceedings of the 12th World Conference on Earthquake Engineering*.

ASCE, A. (2010). Minimum design loads for buildings and other structures, Reston, V.A. U.S.A.

Casapulla, C. (2015), "On the resonance conditions of rigid rocking blocks", *Int. J. Eng. Technol*., **7**(2), 760-771.

Cetin, H., Aydin, E. and Ozturk, B. (2017), "Optimal damper allocation in shear buildings with tuned mass dampers and viscous dampers", *Int. J. Earthq. Impact Eng*., **2**, 89-120. https://doi.org/10.1504/IJEIE.2017.089038.

Cetin, H., Aydin, E. and Ozturk, B. (2019), "Optimal design and distribution of viscous dampers for shear building structures under seismic excitations", *Front. Built Environ*., **5**, 1-13. https://doi.org/10.3389/fbuil.2019.00090.

Code, U.B. (1997), UBC-97, Structural Engineering Design Provisions, International conference of building officials, Whittier, California. U.S.A.

Costanzo, S., D'Aniello, M. and Landolfo, R. (2018), "The influence of moment resisting beam-to-column connections on seismic behavior of chevron concentrically braced frames", *Soil Dyn. Earthq. Eng*., **113**, 136-147. https://doi.org/10.1016/j.soildyn.2018.06.001.

Deierlein, G.G., A.B. Liel, C.B. Haselton and C.A. Kircher (2007), "Assessing building system collapse performance and associated requirements for seismic design". SEAOC convention (Tahoe, CA).

FEMA, F. (1997). "NEHRP guidelines for the seismic rehabilitation of buildings, Federal Emergency Management Agency Washnigton, DC".

FEMA, F.E.M.A. (2009). "Quantification of building seismic performance factors, Washington, D.C", U.S.A.

Ghowsi, A.F. and Sahoo, D.R. (2013), "Seismic performance of buckling-restrained braced frames with varying beam-column connections", *Int. J. Steel Struct*., **13**(4), 607-621. https://doi.org/10.1007/s13296-013-4003-0.

Guan, X., Burton, H. and Moradi, S. (2018), "Seismic performance of a self-centering steel moment frame building: From component-level modeling to economic loss assessment", *J. Construct. Steel Res*., **150**, 129-140. https://doi.org/10.1016/j.jcsr.2018.07.026.

Hamidia, M., Filiatrault, A. and Aref, A. (2014), "Simplified seismic sidesway collapse capacity-based evaluation and design of frame buildings with linear viscous dampers", *J. Earthq. Eng*., **18**(4), 528-552. https://doi.org/10.1080/13632469.2013.876948.

Hessabi, R.M., Mercan, O. and Ozturk, B. (2017), "Exploring the effects of tuned mass dampers on the seismic performance of structures with nonlinear base isolation systems", *Earthq. Struct*., **12**(3), 285-296. https://doi.org/10.12989/eas.2017.12.3.285.

Hoveidae, N. (2019), "Multi-material core as self-centering mechanism for buildings incorporating BRBs", *Earthq. Struct*., **16**(5), 589-599. https://doi.org/10.12989/eas.2019.16.5.589.

He, Z., Wang, Z. and Zhang, Y. (2018), "Collapse safety margin and seismic loss assessment of RC frames with equal material cost", *Struct. Des. Tall Spec. Build*., **27**(1), e1407. https://doi.org/10.1002/tal.1407.

IBC, I. (2006), "International building code", International Code Council, Inc. (formerly BOCA, ICBO and SBCCI) 4051: 60478-65795.

Ibrahim, Y.E. and El-Shami, M.M. (2011), "Seismic fragility curves for mid-rise reinforced concrete frames in Kingdom of Saudi Arabia", *IES J. Part A: Civil Struct.Eng.*, **4**(4), 213-223. https://doi.org/10.1080/19373260.2011.609325.

Juni, P., Gupta, S. and Patel, V. (2017), "Nonlinear dynamic time history analysis of multistoried RCC residential G+23 building for different seismic intensities", *Int. J. Eng. Res. Sci*., **3**(3), 1-8.

Kammula, V., Erochko, J., Kwon, O.S. and Christopoulos, C. (2014), "Application of hybrid-simulation to fragility assessment of the telescoping self-centering energy dissipative bracing system", *Earthqu. Struct. Dyn*., **43**(6), 811-830. https://doi.org/10.1002/eqe.2374.

Karamanci, E. and Lignos, D.G. (2014), "Computational approach for collapse assessment of concentrically braced frames in seismic regions", *J. Struct. Eng*. **140**(8), A4014019. https://doi.org/10.1061/(ASCE)ST.1943-541X.0001011.

Kassem, M.M., Nazri, F.M. and Farsangi, E.N. (2019), "On the quantification of collapse margin of a retrofitted university building in Beirut using a probabilistic approach", *Eng. Sci. Technol., Int. J*., **15**(5) https://doi.org/10.1016/j.jestch.2019.05.003.

Kim, J. and Choi, H. (2004), "Behavior and design of structures with buckling-restrained braces", *Eng. Struct*., **26**(6), 693-706.

Kim, J. and Kim, S. (2017), "Performance-based seismic design of staggered truss frames with friction dampers", *Thin-Walled Struct*., **111**, 197-209. https://doi.org/10.1016/j.tws.2016.12.001.

Kitayama, S. and Constantinou, M.C. (2016), "Design and analysis of buildings with fluidic self-centering systems", *J. Struct. Eng*., **142**(11), 04016105. https://doi.org/10.1061/(ASCE)ST.1943-541X.0001583.

Khorami, M., Alvansazyazdi, M., Shariati, M., Zandi, Y., Jalali, A. and Tahir, M. (2017), "Seismic performance evaluation of buckling restrained braced frames (BRBF) using incremental nonlinear dynamic analysis method (IDA)", *Earthq. Struct*., **13**(6), 531-538. http://www.dspace.uce.edu.ec/handle/25000/14271.

Lavan, O. (2015), "Optimal design of viscous dampers and their supporting members for the seismic retrofitting of 3D irregular frame structures", *J. Struct. Eng*., **141**(11), 04015026. https://doi.org/10.1061/(ASCE)ST.1943-541X.0001261.

Losanno, D., Hadad, H.A. and Serino, G. (2017), "Seismic behavior of isolated bridges with additional damping under far-field and near fault ground motion", *Earthq. Struct*., **13**(2), 119-130. https://doi.org/10.12989/eas.2017.13.2.119.

Maley, T.J., Sullivan, T.J. and G.D. Corte (2010), "Development of a displacement-based design method for steel dual systems with buckling-restrained braces and moment-resisting frames", *J. Earthq. Eng*., **14**(S1), 106-140. https://doi.org/10.1080/13632461003651687.

Manie, S., Moghadam, A.S. and Ghafory-Ashtiany, M. (2015), "Collapse behavior evaluation of asymmetric buildings subjected to bi-directional ground motion", *Struct. Des. Tall Spec. Build*., **24**(8), 607-628. https://doi.org/10.1002/tal.1202.

Putrajaya: Department of Standards Malaysia (2017), Malaysia National Annex to MS EN 1998-1:2017, Eurocode 8: Design of structures for earthquake resistance- Part 1: General Rules, seismic actions and rules for buildings.

Marko, J., Thambiratnam, D. and Perera, N. (2004), "Influence of damping systems on building structures subject to seismic effects", *Eng. Struct*., **26**(13), 1939-1956. https://doi.org/10.1016/j.engstruct.2004.07.008.

Montgomery, M. and Christopoulos, C. (2014), "Experimental validation of viscoelastic coupling dampers for enhanced dynamic performance of high-rise buildings", *J. Struct. Eng*., **141**(5), 04014145. https://doi.org/10.1061/(ASCE)ST.1943-541X.0001092.

Ou, X.Y., He, Z. and Ou, J.P. (2014), "Parametric study on collapse margin ratio of structure", *J.Central South Univ.*, **21**(6), 2477-2486. https://doi.org/10.1007/s11771-014-2202-2.

Ou, X.Y., He, Z. and Ou, J.P. (2014), "Seismic collapse margin of structures using modified mode-based global damage model",

Qamaruddin, S. (2017), "Seismic response study of multi-storied reinforced concrete building with fluid viscous dampers", M.E Dissertation, Chaitanya Bharathi Institute of Technology, India.

Sani, H.P., Gholhaki, T.J. and Banazadeh, M. (2017), "Seismic performance assessment of isolated low-rise steel structures based on loss estimation", *J. Perform. Construct. Facilities*, **31**(4), 04017028. https://doi.org/10.1061/(ASCE)CF.1943-5509.0001028.

Seo, C.Y., Karavasilis, T.L., Ricles, J.M and Sause, R. (2014), "Seismic performance and probabilistic collapse resistance assessment of steel moment resisting frames with fluid viscous dampers." *Earthq. Eng. Struct. Dyn*., **43**(14): 2135-2154.

Shinozuka, M., Feng, M., Kim, H., Uzawa, T. and Ueda, T. (2003), "Statistical analysis of fragility curves. Report." Multidisciplinary Center for Earthquake Engineering Research, MCEER-03-0002.

Silwal, B., Ozbulut, O.E. and Michael, R.J. (2016), "Seismic collapse evaluation of steel moment resisting frames with superelastic viscous damper", J. Construct. Steel Res., **126**, 26-36. https://doi.org/10.1016/j.jcsr.2016.07.002.

Soong, T.T. and Spencer Jr, B.F (2002), "Supplemental energy dissipation: state-of-the-art and state-of-the-practice", *Eng. Struct*., **24**(3), 243-259. https://doi.org/10.1016/S0141-0296(01)00092-X.

Sun, Q., Bo, J., and Dias, D. (2019), "Viscous damping effects on the seismic elastic response of tunnels in three sites", *Geomech. Eng*., **18**(6), 639-650. https://doi.org/10.12989/gae.2019.18.6.639.

Symans, M., Charney, F., Whittaker, A., Constantinou, M., Kircher, C., Johnson, M. and McNamara, R. (2008), "Energy dissipation systems for seismic applications: current practice and recent developments", *J. Struct. Eng*., **134**(1), 3-21. https://doi.org/10.1061/(ASCE)0733-9445(2008)134:1(3).

Terán-Gilmore, A., Ruiz-García, J. and Bojórquez-Mora, E (2015), "Flexible frames as self-centering mechanism for buildings having buckling-restrained braces", *J. Earthq. Eng*., **19**(6), 978-990.

Teran-Gilmore, A. and Virto, N. (2009), "Displacement-based preliminary design of low-rise buildings stiffened with buckling-restrained braces", *Earthq. Spectra*, **25**, 185-211.

Tohidian, M and Manafpour, A (2015), "Evaluation of collapsed margin for RC frames designed based on Iranian seismic code", *7th International Conference on Seismology & Earthquake Engineering.*

Tubaldi, E., Barbato, M. and Dall'Asta, A. (2015), "Efficient approach for the reliability-based design of linear damping devices for seismic protection of buildings", ASCE-ASME *J. Risk Uncert. Eng. Syst., Part A: Civil Eng,*, **2**(2), C4015009. https://doi.org/10.1061/AJRUA6.0000858.

Vamvatsikos, D. and Cornell, C.A (2002), "Incremental dynamic analysis", *Earthq. Eng. Struct. Dyn*., **31**(3), 491-514. https://doi.org/10.1002/eqe.141.

Vision (2000), Performance Based Seismic Engineering of Buildings: pt. 3. Preliminary Northridge lessons. pt. 4. Moving the blue book toward performance-based engineering, Structural Engineers Association of California.

Wongpakdee, N. and Leelataviwat, S. (2017). "Influence of column strength and stiffness on the inelastic behavior of strong-column-weak-beam frames", *J. Struct. Eng*., **143**(9), 04017124. https://doi.org/10.1061/(ASCE)ST.1943-541X.0001864.

Xie, Q. (2005), "State of the art of buckling-restrained braces in Asia", *J. Construct. Steel Res*., **61**(6), 727-748. https://doi.org/10.1016/j.jcsr.2004.11.005.

Xu, Z.D., Shen, Y.P. and Zhao, H.T. (2003), "A synthetic optimization analysis method on structures with viscoelastic dampers", *Soil Dyn. Earthq. Eng*., **23**(8), 683-689. https://doi.org/10.1016/j.soildyn.2003.07.003.

Yang, Y., Liu, R., Xue, Y. and Li, H. (2017), "Experimental study on seismic performance of reinforced concrete frames retrofitted with eccentric buckling-restrained braces (BRBs)", *Earthq. Struct*., **12**(1), 79-89. https://doi.org/10.12989/eas.2017.12.1.079.

Zhang, L., Su, M., Zhang, C., Shen, H., Islam M.M. and Zhang, R. (2019), "A design method of viscoelastic damper parameters based on the elastic-plastic response reduction curve", *Soil Dyn. Earthq. Eng*., **117**, 149-163. https://doi.org/10.1016/j.soildyn.2018.09.050.

Zhu, S. and Zhang, Y. (2008), "Seismic analysis of concentrically braced frame systems with self-centering friction damping braces", *J. Struct. Eng*., **134**(1), 121-131. https://doi.org/10.1061/(ASCE)0733-9445(2008)134:1(121).

CC